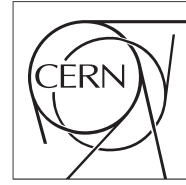


The Compact Muon Solenoid Experiment
Conference Report

Mailing address: CMS CERN, CH-1211 GENEVA 23, Switzerland



31 October 2024 (v3, 07 November 2024)

Radiation and magnetic field qualification of LVPS - a unified 12V DC power source for the CMS detector.

Krzysztof Stachon, Guenther Dissertori, Tomasz Gadek, Werner Lustermann for the CMS Collaboration

Abstract

Efforts aiming at consolidating the powering for the CMS detector have led to the development of a Low Voltage Power Supply (LVPS). The LVPS converts 380 V DC to 12 V DC, suitable for powering the widely used bPOL12V point-of-load DC-DC converter. To limit cable size, the LVPS must be hosted in the CMS experimental cavern, being exposed to ionizing radiation and stray magnetic field of up to 120 mT. The device is made of Commercial Off-The-Shelf (COTS) components, therefore, thorough qualifications at various design stages were performed to ensure its reliable operation in the harsh environmental conditions for the HL-LHC era.

Presented at *TWEPP2024 Topical Workshop on Electronics for Particle Physics*

1 PREPARED FOR SUBMISSION TO JINST

2 TOPICAL WORKSHOP ON ELECTRONICS FOR PARTICLE PHYSICS - TWEPP 2024
3 30 SEPTEMBER - 4 OCTOBER 2024
4 GLASGOW, UK

5 **Radiation and magnetic field qualification of LVPS -** 6 **a unified 12V DC power source for the CMS detector.**

7 **K. Stachon^{a,1} , G. Dissertori^a , T. Gadek^{a,b} , W. Lustermann^a on behalf of the CMS**
8 **Collaboration**

9 ^a*Institute for Particle Physics and Astrophysics, ETH Zurich,*
10 *Otto-Stern-Weg 5, 8093 Zurich, Switzerland*

11 ^b*Advanced Power Semiconductor Laboratory,*
12 *Physikstrasse 3, 8092 Zurich, Switzerland*

13 *E-mail: krzysztof.stachon@proton.me*

14 **ABSTRACT:** Efforts aiming at consolidating the powering for the CMS detector have led to the
15 development of a Low Voltage Power Supply (LVPS). The LVPS converts 380 V DC to 12 V DC,
16 suitable for powering the widely used bPOL12V point-of-load DC-DC converter. To limit cable
17 size, the LVPS must be hosted in the CMS experimental cavern, being exposed to ionizing radiation
18 and stray magnetic field of up to 120 mT. The device is made of Commercial Off-The-Shelf (COTS)
19 components, therefore, thorough qualifications at various design stages were performed to ensure
20 its reliable operation in the harsh environmental conditions for the HL-LHC era.

21 **KEYWORDS:** Voltage distributions; Modular electronics; Radiation-hard electronics

¹Corresponding author.

22 **1 Introduction**

23 The CMS Phase-2 Upgrade [1, 2] on-detector electronics require operational voltage levels ranging
24 typically from 1.2 V to 2.5 V DC. Electrical power is delivered from the power grid to the Point-of-
25 Load (POL) via three intermediate voltage conversion stages. The first stage converts three-phase
26 230 V AC into 380 V DC using a Commercial off-the-shelf (COTS) AC-DC power conversion
27 system [3]. The second stage uses Low Voltage Power Supply (LVPS) to step-down from 380 V DC
28 to 12 V DC, the input voltage required by the POL converters. The LVPS are located in the CMS
29 experimental cavern approximately 30 m away from the on-detector electronics in a moderately
30 harsh radiation and magnetic field environment. The third stage employs CERN’s radiation tolerant
31 bPOL12V[4, 5] and linPOL12V converter ASICs, embedded into the on-detector electronics.

32 **1.1 LVPS – Low Voltage Power Supply.**

33 The LVPS must operate in the radiation and magnetic field of the CMS experimental cavern with a
34 required tolerance of up to 32 Gy Total Ionizing Dose (TID), 2×10^{11} HEH cm^{-2} (>20 MeV) High
35 Energy Hadron Fluence (HEH), and 1×10^{13} n cm^{-2} (1 MeV equivalent) neutron fluence. This will
36 cover expected radiation levels during the HL-LHC era with margin, corresponding to integrated
37 luminosity of 4000 fb^{-1} . Furthermore, the device must remain operational in the presence of an
38 external static magnetic field of up to 120 mT.

39 The development and production of the LVPS have been outsourced by CERN to industry.
40 Nonetheless, we implemented rigorous monitoring to ensure compliance with specifications. In
41 addition, we conducted radiation and magnetic-field evaluations on prototypes. The outcomes of
42 these evaluations are presented in this manuscript.

43 The LVPS feature an input voltage ranging from 342 V to 400 V DC and output voltages
44 ranging from 7 V to 13 V DC. The LVPS building block is a 720 W module with up to ten of them
45 fitting a 5U tall 19” chassis, featuring water cooling. A modular design, allows for 3 different
46 module configurations: 12 channels of 60 W, 6 channels of 120 W, or 3 channels of 240 W. Each
47 module in the chassis is individually remote controlled using CAN-BUS. All module outputs are
48 individually protected by dedicated, redundant over-voltage protection, ensuring output voltages
49 are staying below an adjustable threshold. This additional protection was introduced to protect
50 bPOL12V against voltage transients.

51 Three CMS sub-detectors joined in a common procurement project requiring about 1000
52 modules, corresponding to 720 kW total output power.

53 **2 Radiation qualification**

54 **2.1 Qualification strategy**

55 The LVPS is designed using COTS components. While this methodology significantly reduces
56 cost, it requires thorough radiation testing during the development phase, as electronic components
57 typically deviate from their specified performance parameters when irradiated. The damage is
58 caused by several effects of ionising radiation, such as Total Ionizing Dose (TID), displacement
59 damage and Single Event Effect (SEE). The latter two can originate as well from hadron-induced
60 damage. SEEs are special as a single interaction can potentially damage an electronic components

61 or induce errors within digital electronics. In power electronics components, the most critical effect
 62 is Single Event Burnout (SEB), caused by radiation-induced breakdowns in power transistors [6].

63 The LVPS development started with component selection for gate drivers, Analog-to-Digital
 64 Converters (ADCs), and Digital-to-Analog Converters (DACs), using CERN’s radiation working
 65 group [7] database, and component-level radiation screening tests at Paul Scherrer Institute (PSI)’s
 66 Proton Irradiation Facility (PIF). Subsequently, system-level tests were conducted at the CERN’s
 67 CHARM mixed-field irradiation facility, providing conditions as found in the experiments. These
 68 tests were meticulously prepared and executed by us, while the Device Under Tests (DUTs) have
 69 been supplied by the development contractor: Kontron HARTMANN-WIENER.

70 **2.2 Results**

71 Since 2021, five irradiation campaigns have been completed. The result of the three most recent
 72 ones, including testing of full prototypes: Prototype-I and Prototype-II, are reported below.

73 **2.2.1 June 2023 test at CHARM**

74 The goal of this test was the evaluation of the Over-Current Protection (OCP) circuit, and of the
 75 micro-controller including Controller Area Network (CAN) communication.

76 The microcontroller was tested by sending a series of queries every second. The communication
 77 was stable throughout the test, except one case, where a query missed the response. This was not
 78 considered a problem, because all subsequent queries were answered correctly.

79 The OCP circuit comprises a current measurement shunt resistor (100 mΩ), followed by a
 80 differential amplifier, and a latching comparator with threshold and RESET inputs, and over-current
 81 protection signal (V_{OCP}) output (figure 1). It was evaluated by controlling the voltage across
 82 the shunt resistor, creating a cyclic current test pattern (figure 2) of 60 s duration. The current
 83 first crosses the threshold trigger the comparator, then it is lowered just below the threshold, the
 84 comparator is reset, and V_{OCP} is monitored checking for spurious triggers. Two test boards with
 85 two sets of components have been tested: set A hosting amplifier: Onsemi LM358D, comparator:
 86 Onsemi LM293M, and set B hosting amplifier and comparator: MC34072.

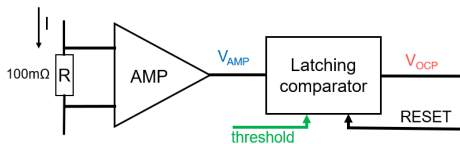


Figure 1: Schematic view of OCP circuit.

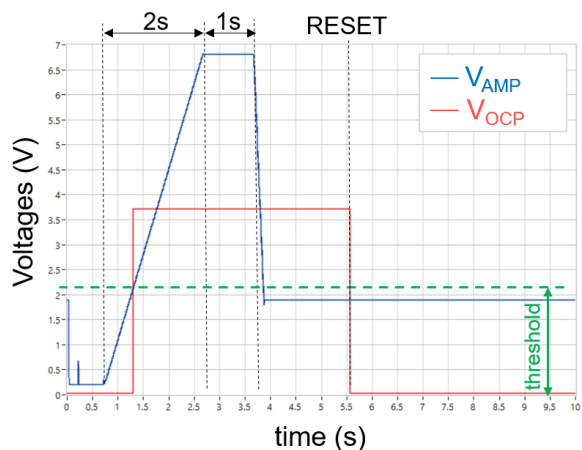


Figure 2: One cycle of the OCP test pattern with typical amplifier and latching comparator outputs.

87 Previous tests revealed the presence of radiation-
 88 induced spurious OCP tripping. In this test, all compara-
 89 tors output voltages were sampled with 600 kS/s enabling
 90 waveform reconstruction. This revealed that spikes are
 91 permanently present and have a typical waveform (figure
 92 3) that may be filtered out. Moreover, a small drifts of the
 93 comparator thresholds was measured (figure 4), with test
 94 set A performing, slightly better showing a total drift of
 95 1.3 % at 32 Gy TID.

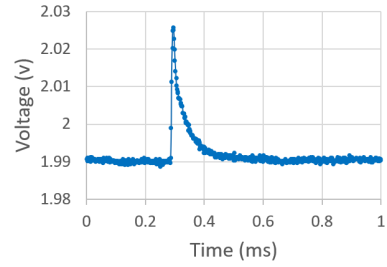


Figure 3: Typical radiation-induced spike.

96 **2.2.2 October 2023 test at CHARM**

97 Prototype-I, was evaluated at CERN Highly-Accelerated Mixed Field Facility (CHARM) for two
 98 weeks. The setup comprised a chassis and three modules, one per configuration, 12, 6, and
 99 3-channel. During the test all input and output voltages and currents of all 21 channels were
 100 continuously monitored at 50% of full load, and every three hours a test sequence was executed,
 101 including input power cycling, idle current measurement, OCP test, efficiency measurements and
 102 more. All output voltage remained stable (figure 5), with minor radiation-induced few mV jumps.
 103 Figure 6 shows the exceptional occurrence of a 25 mV jump.

104 All three modules failed to boot at TIDs between 30 Gy and 47 Gy. The root cause was traced
 105 to the LM317 linear regulator, which had been sourced from a different manufacturer than specified.
 106 Moreover, CAN communication was intermittently lost, although rebooting resolved the issue. One
 107 channel failed at a TID of 100 Gy, 3-times higher than required.

108 **2.2.3 June 2024 test at CHARM**

109 Prototype-II was tested at CHARM for two weeks. Issues identified in Prototype-I had been
 110 resolved. However, a new problem was discovered. The output current measurement is drifting

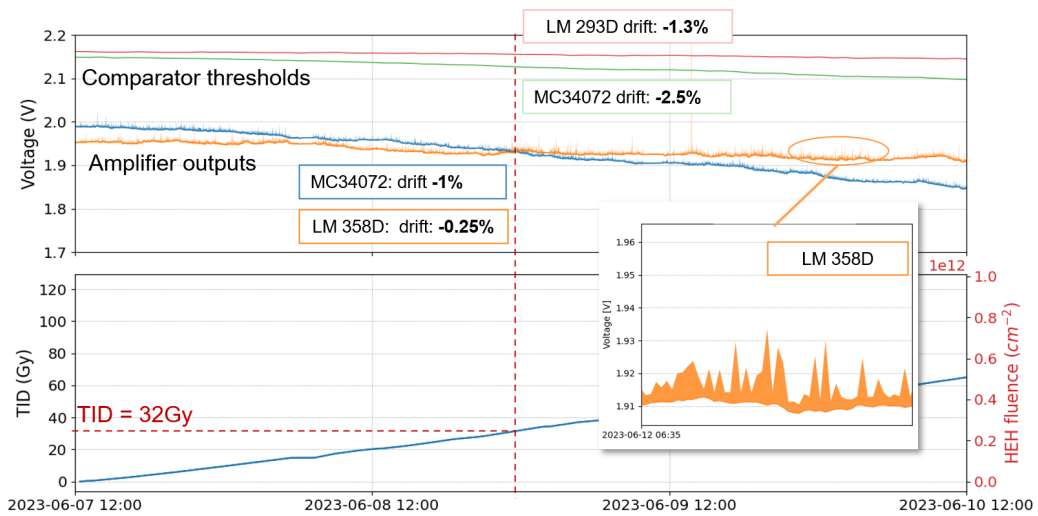


Figure 4: OCP circuit amplifier and compactor drifts versus TID at constant input current.

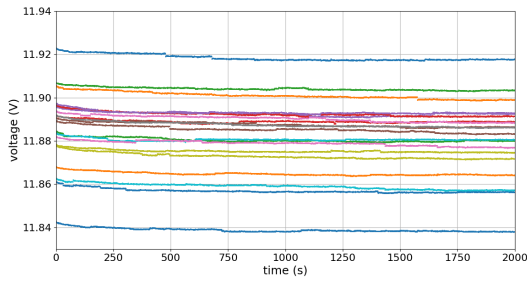


Figure 5: Typical voltage waveform for 21 channels tested. Acquired at 30 Gy.

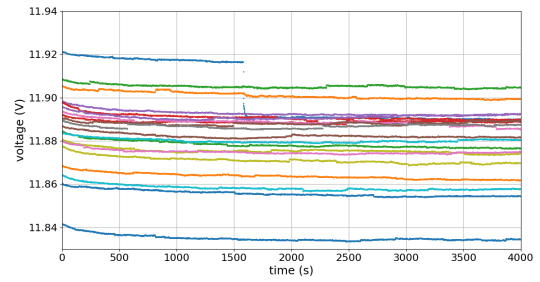


Figure 6: Voltage jump registered at 35 Gy in one channel (blue) out of 21 tested.

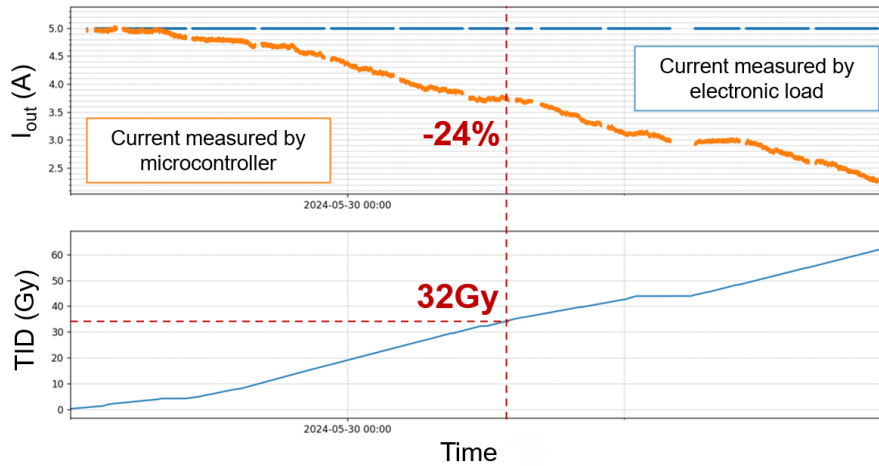


Figure 7: Drift of output current measurement (orange) with 5 A constant load (blue), typical channel.

111 significantly as a function of TID, resulting in 20 % to 40 % deviation from the trues. See figure 7
 112 for a typical channel. This compromises the OCP feature.

113 Additionally, SEEs caused failures of the ADuM3152ARSZ digital isolators, rendering the
 114 concerned channel not controllable. One such failure had been observed in the previous test while
 115 this time 5 out of 21 channels were affected. However, the channels were exposed to over 5 times
 116 higher HEH fluence than the lifetime exposure. We estimate the upper limit cross-section $\hat{\sigma}$ for this
 117 failure with 95% confidence level following reference [8]: $\hat{\sigma} = \frac{\chi_{2(d+1),0.95}^2}{2 \sum_{i=1}^N \Phi_i} \approx 3.29 \times 10^{-14} \text{ cm}^2$, with N
 118 being the number of devices, d the number of observed failures, and Φ_i the fluence received by device
 119 i, $i = 1 \dots N$. Although the cross-section is relatively low, it was decided to mitigate the problem
 120 by replacing the component with a combination of other digital isolators: ADUM3401BRWZ and
 121 ADUM3402BRWZ.

122 3 Magnetic field qualification

123 In November 2023 Prototype-I was tested in a magnet. We measured efficiency as function of
 124 the external magnetic field in a range from 0 mT to 153 mT in three orthogonal orientations. The
 125 expected minimum LVPS efficiency for loads >40% of full load is 88%. Satisfactory performance
 126 was observed solely in one orientation (figure 8), whereas the other orientations (figures 9, 10)

127 exhibited considerable efficiency degradation attributable to the magnetic field. Subsequent in-
 128 vestigations identified a transformer fitted with a magnetic shield as the root cause. The shield,
 129 manufactured from high-purity iron, had not been subjected to thermal annealing post-machining.
 130 Computational simulations using COMSOL indicated that thermal annealing significantly enhances
 131 the performance of the shield, sufficient to cure the observed problem.

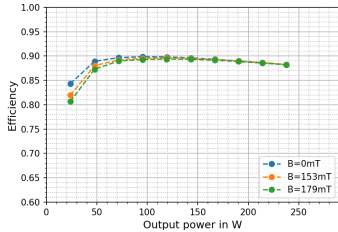


Figure 8: X orientation.

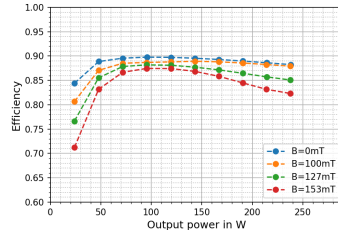


Figure 9: Y orientation

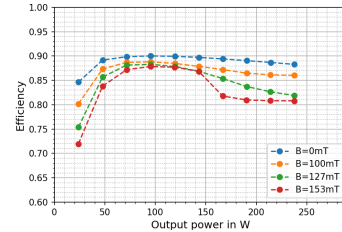


Figure 10: Z orientation

132 4 Summary and Conclusions

133 Comprehensive radiation and magnetic field qualification of newly developed LVPSs were per-
 134 formed on both components and full prototypes. The tests demonstrated the viability of the LVPSs
 135 prototypes for the CMS detector under HL-LHC conditions in the specified, harsh radiation and
 136 magnetic field environment.

137 Key findings of the radiation tests are: The LVPSs voltage regulation is stable, with minor, non-
 138 critical radiation-induced voltage jumps. There are radiation-induced spikes in the OCP circuitry,
 139 but due to its consistent shape, these will be filtered out. Dose-related boot failures and occasional
 140 CAN communication losses were observed. They were either mitigated or occurred beyond the
 141 specified TID. The use of COTS components posed severe challenges, particularly in maintaining
 142 the robustness of regulators such as the LM317, highlighting the importance of strict component
 143 sourcing and thorough qualification.

144 Magnetic field tests revealed orientation-dependent efficiency degradation. Electromagnetic
 145 simulations suggested that thermal annealing of the magnetic shield would alleviate these ineffi-
 146 ciencies and extend the operational performance of the LVPS. Consequently, the magnetic shield
 147 of all future LVPS, prototypes, and production, will be thermally annealed.

148 Overall, the LVPS has demonstrated strong potential, and with the identified issues addressed
 149 in future iterations, it is well on its way to meeting the operational requirements of CMS at the
 150 HL-LHC. The next and likely final iteration will feature improved current measurement accuracy
 151 and specified performance in all magnetic field orientations.

152 Acknowledgments

153 The authors thank Michael Dröge and Christian Haller from ETH Zurich for their invaluable support
 154 in preparing and installing the tests setups, and the Kontron HARTMANN- WIENER engineers,
 155 for providing the DUTs, and their contributions to the preparation of the June 2024 radiation test.
 156 This work was supported by the Swiss National Science Foundation, SNF FLARE 201476 grant.

